ANALYSIS OF TARGET DETECTION VIA MATRIX COMPLETION

Sunav Choudhary and Urbashi Mitra

Ming Hsieh Department of Electrical Engineering
University of Southern California, Los Angeles, CA-90089
{sunavcho,ubli}@usc.edu

ABSTRACT

A problem of broad interest is the detection and localization of a target or object from its generated field. In this paper, a detection and localization strategy which exploits the structure of target fields is designed and analyzed. In taking advantage of this structure, one is able to reduce sample complexity requirements while maintaining good performance. In particular, an exploration-exploitation approach to target detection is proposed utilizing the theory of low-rank matrix completion for a decaying separable target field. The assumptions on the field are fairly generic and are applicable to many decay profiles. Our approach does not require specific knowledge of the field, only that it admits a rank-one representation. A performance analysis for localization is presented that characterizes a trade-off with sample complexity in the presence of noise.

Index Terms— target detection, localization, rank-one matrix completion, side-scan sonar, exploration-exploitation tradeoff

1. INTRODUCTION

Target detection from samples of a field, is a generic problem of interest in a wide variety of applications including environmental monitoring, cyber-security, medical diagnosis and military surveillance. The ubiquity and importance of this problem has led to the development of a rich literature utilizing ideas from statistics, signal processing, information theory, machine learning and data mining, and addressing numerous application specific variations. In this paper, we shall consider the problem of target detection and localization from highly incomplete samples of the target field. As a simple illustrative example, consider the side-scan sonar image in Figure 1, acquired by an autonomous underwater vehicle (AUV) with the goal of locating the position of the target (marked by region of high intensity reflection) amongst background clutter (reflections from the sea bed). Depending on the specific application, the target fields could be highly structured (as in Figure 1), thus enabling good detection algorithms from an incomplete set of samples of the field, following the philosophy of compressed sensing [1]. Beside theoretical interest, a possibility of reduced sample complexity of target detection is highly beneficial for applications where speed of acquisition is a bottleneck, like magnetic resonance imaging and underwater sonar imaging.

1.1. Contributions

Herein, we shall assume a static *separable* target field whose magnitude decays monotonically with increasing distance from the true location of the target. We employ an approach based on low-rank matrix completion [2] that allows us to derive an algorithm that *does not* need the knowledge of the target field decay profile. In particular, the algorithm can be viewed as a solution to the exploration-exploitation problem wherein the possible location of the target is unknown *a priori* and the sampling strategy enables the coarse learning of the location and presence of target, resulting in subsequent sampling in more informed locations. The main contribution of this paper over our prior works [3, 4] is the development of an analytical trade-off between the sampling complexity and the target localization error in the presence of noise when employing a uniformly random spatial pixel sampling strategy. Our approach is general and as such does not exploit specialized models for the background clutter. Thus, further improvement in performance would be possible by taking this information into consideration. For example, the sonar images of the form in Figure 1 suffer from imaging artifacts.

This research has been funded in part by the following grants and organizations: ONR N00014-09-1-0700, NSF CNS-1213128, AFOSR FA9550-12-1-0215, NSF CCF-1410009, NSF CPS-1446901, DOT CA-26-7084-00 and NSF CCF-1117896.

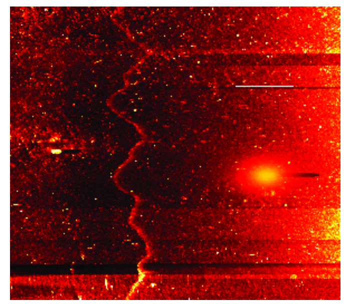

Fig. 1. An underwater side-scan sonar image with pseudo-synthetic target signature. The background noise and artifacts are due to reflections from the seabed.

1.2. Related Work

For an early survey of active target detection, we refer the reader to [5] consisting of statistical and signal processing approaches that assume availability of the *full* target field/signature (see also [6, 7]). The field of anomaly detection [8] further generalizes the scope of target detection and employs tools from machine learning, *e.g.* [9–14] perform window based target detection in *full* sonar images. General theoretical analysis on either of these problems is plagued by the lack of good models for experimental scenarios that are amenable to tractable analysis. In [15–18] there is a focus on path planning for active sensing (in particular, [18] uses compressed sensing) with an explicit consideration of the navigation cost and stopping time, in contrast to the goals of this paper. Early work [19] focusing on target detection in multiple-in-multiple-out (MIMO) radar used a statistical approach, which was refined in [20–22] using a combination of joint sparse sensing and low-rank matrix completion ideas, relying on the strong theoretical guarantees of low-rank matrix completion from random samples [2,23,24]. The focus in the papers [20–22] is to adapt the design of the MIMO radar array to optimize coherence, which is also very different from our goal here of studying the detection and localization error performance of low-rank matrix completion. Finally, we note that distilled sensing [25–27] has a somewhat similar algorithmic philosophy as ours for target detection but therein the field is assumed to be sparse rather than low-rank, thus facing basis mismatch challenges that we can avoid completely.

1.3. Notation and Organization

We use lowercase boldface alphabets to denote column vectors (*e.g.* $\boldsymbol{z}$) and uppercase boldface alphabets to denote matrices (*e.g.* $\boldsymbol{A}$). The MATLAB® indexing rules will be used to denote parts of a vector/matrix (e.g. $\boldsymbol{A}(2:3,4:6)$ denotes the sub-matrix of $\boldsymbol{A}$ formed by the rows $\{2,3\}$ and columns $\{4,5,6\}$). The all zero, all one and identity matrices shall be respectively denoted by $\mathbf{0}$, $\mathbf{1}$ and $\mathbf{I}$ with dimensions dictated by context. $(\cdot)^{\mathrm{T}}$ denotes the transpose operation and $\langle\cdot,\cdot\rangle$ denotes the standard inner product on $\mathbb{R}^n$. The functions $\|\cdot\|_{\mathrm{F}}$ and $\|\cdot\|_*$ respectively return the Frobenius and nuclear norms of their matrix argument. The function $|\cdot|$ applied to a scalar (repectively a set) returns its absolute value (respectively cardinality). $\mathbb{R}$ and $\mathbb{Z}_+$ respectively denote the set of real numbers and the set of positive integers. We shall use the $O(\cdot)$, $\Omega(\cdot)$ and $\Theta(\cdot)$ notations to denote order of growth for functions.

Rest of the paper is organized as follows. Section 2 formulates the problem by stating our assumptions on the target field and demonstrating its rank one nature. Section 3 describes our sampling and localization approach and develops a performance analysis for the same in the presence of noise. Localization bounds are developed as a function of signal-to-noise ratio (SNR) and sample complexity and numerically demonstrated. Section 4 concludes the paper.

2. PROBLEM DESCRIPTION

2.1. Target Field Assumptions

We shall closely follow the system model described in [3]. Let the search region (see Figure 1) be the two dimensional unit square, and $\boldsymbol{y}=(y_{\mathrm{c}},y_{\mathrm{r}})\in[0,1]^2$ denote an arbitrary location in the search space. Let $H\colon\mathbb{R}^2\to\mathbb{R}$ denote the *scalar valued* target signature. We shall make the following key assumptions on the field $H(\boldsymbol{y})$:

(A1) $H(\boldsymbol{y})$ is separable in some known basis of $\mathbb{R}^2$, independent of the true location of the target.

(A2) The magnitude of the field, $|H(\boldsymbol{y})|$ is a monotonically non-increasing function of the distance from the target in every direction.

(A3) $H(\boldsymbol{y})$ is spatially invariant relative to the target's position.

We assume separability of $H(\boldsymbol{y})$ in the y_{c} and y_{r} directions (*i.e.* in the canonical basis $\{[1,0],[0,1]\}$) as per (A1). This means that there exist functions $F\colon\mathbb{R}\to\mathbb{R}$ and $G\colon\mathbb{R}\to\mathbb{R}$ such that $H(\boldsymbol{y})=F(y_{\mathrm{c}})G(y_{\mathrm{r}})$, $\forall(y_{\mathrm{c}},y_{\mathrm{r}})\in\mathbb{R}^2$. Assumption (A2) is intuitively clear and can be mathematically described by the inequality:

$$|H(t_1(\boldsymbol{y}-\boldsymbol{y}_0))|\geq|H(t_2(\boldsymbol{y}-\boldsymbol{y}_0))|, \tag{1}$$

holding $\forall\boldsymbol{y}\in\mathbb{R}^2, t_2>t_1>0$, where $\boldsymbol{y}_0$ represents the unknown location of the target. Assumption (A3) implies that if the target were moved from $\boldsymbol{y}_0$ to a new position $\boldsymbol{y}_0'$, then the new field at location $\boldsymbol{y}$ would be given by $H(\boldsymbol{y}-\boldsymbol{y}_0'+\boldsymbol{y}_0)$, thus ensuring that (A1) holds in the canonical basis, regardless of the target's position $\boldsymbol{y}_0$.

Scalar fields commonly correspond to intensity measurements (like the sonar image in Figure 1). The following types of commonly assumed intensity fields satisfy our assumptions:

1. Exponential fields: $H(\boldsymbol{y})=H_0\exp\left(-\|\boldsymbol{\Sigma}\boldsymbol{y}\|_p^p\right)$, for any 2×2 diagonal matrix $\boldsymbol{\Sigma}\in\mathbb{R}^{2\times2}$ and constants $p,H_0>0$. For $p=1$ and $p=2$, we respectively get two dimensional Laplacian and Gaussian fields.
2. Power Law fields:
$$H(\boldsymbol{y})=H_0(a_1+|y_{\mathrm{c}}|^{p_1})^{-r_1}(a_2+|y_{\mathrm{r}}|^{p_2})^{-r_2} \tag{2}$$
for constants $H_0,p_1,p_2,a_1,a_2,r_1,r_2>0$. With $p_1=p_2=2$ and $r_1=r_2=1$, we get a field that is separable as a product of two Cauchy fields $H(\boldsymbol{y})=H_0\left(a_1+y_{\mathrm{c}}^2\right)^{-1}\left(a_2+y_{\mathrm{r}}^2\right)^{-1}$.
3. Any *multiplicative* combination of fields satisfying our assumptions, *e.g.*
$$H(\boldsymbol{y})=H_0\frac{\exp\left(-c_1y_{\mathrm{c}}^2-c_2|y_{\mathrm{r}}|\right)}{(1+|y_{\mathrm{c}}|)(1+y_{\mathrm{r}}^2)} \tag{3}$$
for some constants $H_0,c_1,c_2>0$. In particular, the set of separable fields is closed under multiplication.

2.2. Formulation

By virtue of assumption (A2), detecting the target is synonymous with locating the peak of the induced field. In light of our assumptions, we can state the target detection problem as the following task: *To determine the location of the peak in the field $H(\boldsymbol{y})$ from its values in only a few locations $\boldsymbol{y}\in[0,1]^2$.* We'll use the *lifting* technique from optimization [28] to demonstrate that the separability assumption (A1) implies a rank one structure on the field. This key observation allows large reductions in sample complexity for target detection by utilizing existing theoretical results for high-dimensional low-rank matrix completion algorithms [2,23].

Let $H(\boldsymbol{y})=F(y_{\mathrm{c}})G(y_{\mathrm{r}})$ be the canonical separable representation of the target field and let $\boldsymbol{H}$ denote a high resolution discretized version of $H(\boldsymbol{y})$ on the $n\times n$ regular grid $\mathcal{V}\in[0,1]^2$. Let $\mathcal{V}=\left\{y_{\mathrm{r}}^1,y_{\mathrm{r}}^2,\ldots,y_{\mathrm{r}}^n\right\}\times\left\{y_{\mathrm{c}}^1,y_{\mathrm{c}}^2,\ldots,y_{\mathrm{c}}^n\right\}$ be the representation of the grid for $y_{\mathrm{r}}^1,y_{\mathrm{r}}^2,\ldots,y_{\mathrm{r}}^n,y_{\mathrm{c}}^1,y_{\mathrm{c}}^2,\ldots,y_{\mathrm{c}}^n\in[0,1]$. The set of all possible sampled values of the field on the set $\mathcal{V}$ is given by $\left\{H\left(y_{\mathrm{c}}^i,y_{\mathrm{r}}^j\right)\,\middle|\,\left(y_{\mathrm{c}}^i,y_{\mathrm{r}}^j\right)\in\mathcal{V}\right\}$ and can be arranged in the form of the rank one matrix $\boldsymbol{H}\in\mathbb{R}^{n\times n}$, whose $(i,j)^{\text{th}}$ entry $\boldsymbol{H}(i,j)$ is

$$\boldsymbol{H}(i,j)=H\left(y_{\mathrm{c}}^i,y_{\mathrm{r}}^j\right)=F\left(y_{\mathrm{c}}^i\right)G\left(y_{\mathrm{r}}^j\right). \tag{4}$$

where $\left(y_{\mathrm{c}}^i,y_{\mathrm{r}}^j\right)$ is the physical location of the $(i,j)^{\text{th}}$ point in $\mathcal{V}$. The matrix $\boldsymbol{H}$ is clearly of rank one since we can express it as the outer product $\boldsymbol{H}=\boldsymbol{f}\boldsymbol{g}^{\mathrm{T}}$ where $\boldsymbol{f}=\left[F\left(y_{\mathrm{c}}^1\right),F\left(y_{\mathrm{c}}^2\right),\ldots,F\left(y_{\mathrm{c}}^n\right)\right]^{\mathrm{T}}$ and $\boldsymbol{g}=\left[G\left(y_{\mathrm{r}}^1\right),G\left(y_{\mathrm{r}}^2\right),\ldots,G\left(y_{\mathrm{r}}^n\right)\right]^{\mathrm{T}}$. Without loss of generality, we assume that both $y_{\mathrm{r}}^1,y_{\mathrm{r}}^2,\ldots,y_{\mathrm{r}}^n$ and $y_{\mathrm{c}}^1,y_{\mathrm{c}}^2,\ldots,y_{\mathrm{c}}^n$ are sorted in ascending order, corresponding respectively to traversing the grid from top to bottom and from left to right. Because of the preceding derivation, we can refer to $\boldsymbol{H}$ as the target field with a slight abuse of terminology. Consequently, we can consider $\mathcal{V}$ in a rescaled sense to refer to the set of index pairs $\{1,2,\ldots,n\}^2$ for the matrix $\boldsymbol{H}$.

3. SAMPLING AND RECONSTRUCTION APPROACH

3.1. The Algorithm

We use a standard low-rank noisy matrix completion followed by a subsequent peak detection with some margin of error. The algorithm starts with n^2 possible locations of the peak and after execution, returns a smaller set of index pairs that are guaranteed to contain the peak, provided the sampling density is high enough. This can be considered as the "first pass" over the search region, giving us a coarse segmentation of the region into an area of interest that contains the peak, and its complement region which can be discarded. The algorithmic procedure can be repeated on this smaller region of interest, giving rise to the *exploration-exploitation* interpretation of our approach. The key steps for the first pass are described below.

Algorithm Inputs:

1. The regular grid $\mathcal{V} = \{1, 2, \ldots, n\}^2$.
2. Upper bound on noise power per sample (averaged across samples), ϵ^2.

Algorithm Output: Localization index bounds $l_c^L, l_c^R, l_r^L, l_r^R \in \mathbb{Z}_+$ such that the target is located within the rectangular region formed by the index pairs in $\left\{l_c^L, l_c^L + 1, \ldots, l_c^R\right\} \times \left\{l_r^L, l_r^L + 1, \ldots, l_r^R\right\}$.

Algorithm Steps:

(S1) Select a subset $\mathcal{V}' \subset \mathcal{V}$ of $O\big(n \log^2 n\big)$ points uniformly and independently at random from the n^2 points in $\mathcal{V}$, and measure the (possibly noisy) samples $\boldsymbol{H}(i,j)$ for every index pair $(i,j) \in \mathcal{V}'$, *i.e.* record the projection $\mathcal{P}_{\mathcal{V}'}(\boldsymbol{H})$.

(S2) Solve the convex nuclear norm heuristic to stable low-rank matrix completion [2]

$$\begin{aligned} \underset{\boldsymbol{Q}}{\text{minimize}} \quad & \|\boldsymbol{Q}\|_* \\ \text{subject to} \quad & \|\mathcal{P}_{\mathcal{V}'}(\boldsymbol{Q}) - \mathcal{P}_{\mathcal{V}'}(\boldsymbol{H})\|_\mathrm{F} \le \epsilon \big|\mathcal{V}'\big|, \end{aligned} \tag{P$_1$}$$

to obtain the solution $\widehat{\boldsymbol{H}} \in \mathbb{R}^{n \times n}$.

(S3) Compute the top singular value and corresponding singular vectors of $\widehat{\boldsymbol{H}}$ as the triplet $(\boldsymbol{u}, \sigma, \boldsymbol{v})$.

(S4) Compute the lower bounding index $l_c^L \in \{1, 2, \ldots, n\}$ for localization as the solution to the optimization problem

$$\begin{aligned} \underset{\boldsymbol{z}, l}{\text{minimize}} \quad & l \\ \text{subject to} \quad & l \in \{1, 2, \ldots, n\}, \\ & \boldsymbol{z}(j+1) \le \boldsymbol{z}(j); \quad j = l, l+1, \ldots, n-1, \\ & \boldsymbol{z}(j-1) \le \boldsymbol{z}(j); \quad j = 2, 3, \ldots, l, \\ & \langle \boldsymbol{z}, \boldsymbol{v} \rangle \ge \|\boldsymbol{z}\|_2 \sqrt{1 - \zeta^2/\sigma^2}, \\ & \boldsymbol{z}(j) \ge 0; \quad j = 1, 2, \ldots, n, \end{aligned} \tag{P$_2$}$$

where ζ is an upper bound on $\big\|\boldsymbol{H} - \widehat{\boldsymbol{H}}\big\|_\mathrm{F}$ form the theory of low-rank matrix completion and depends only on n, ϵ and $|\mathcal{V}'|$ (see Section 3.2). If necessary, replace $\boldsymbol{v}$ by $-\boldsymbol{v}$ in Problem (P$_2$) to make it feasible.

(S5) Compute the upper bounding index $l_c^R \in \{1, 2, \ldots, n\}$ for localization as the solution to Problem (P$_2$) with the objective function changed from l to $-l$.

(S6) Repeat steps (S4) and (S5) with $\boldsymbol{v}$ replaced by $\boldsymbol{u}$ in Problem (P$_2$) to respectively obtain the remaining two indices l_r^L and l_r^R (both in $\{1, 2, \ldots, n\}$).

In the algorithm above, $\mathcal{P}_{\mathcal{V}'}(\cdot)$ denotes the projection operator on the set of index pairs in $\mathcal{V}'$. This algorithm differs from the one presented in [3] on account of the explicit computation of the noise dependent localization bounding region in steps (S4) through (S6). We remark that for every fixed value of $l \in \{1, 2, \ldots, n\}$, it is clear that Problem (P$_2$) reduces to a *convex feasibility problem* [29] and is efficiently solvable. Since l admits at most n distinct values, Problem (P$_2$) as whole is efficiently solvable.

Results from low-rank matrix completion [2, 23] guarantee that the sample complexity of $|\mathcal{V}'| = O\big(n \log^2 n\big)$ is sufficient for a good mean-squared error (MSE) reconstruction of $\boldsymbol{H}$ as the solution to Problem (P$_1$) with high probability (*w.h.p.*) over the realizations of $\mathcal{V}'$, and that the hidden constant depends on the *coherence* [23] of $\boldsymbol{H}$ with the canonical basis for matrices. It is intuitive to reason that a good MSE reconstruction should also lead to a good estimate for peak localization in $\boldsymbol{H}$. Next, we will make this intuition precise.

3.2. Correctness and Localization Performance

We shall assume that the sampling budget $|\mathcal{V}'| = \Omega\big(n \log^2 n\big)$ is sufficient, *i.e.* with the right constants as given by [23] or [2], so that the corresponding result on the MSE of reconstruction holds *w.h.p.* over realizations of $\mathcal{V}'$. In particular, we have a bound on the reconstruction error of the form $\big\|\boldsymbol{H} - \widehat{\boldsymbol{H}}\big\|_\mathrm{F} \le \zeta$ for ζ depending only on n, ϵ and $|\mathcal{V}'|$, where $\hat{\boldsymbol{H}}$ is the solution to Problem (P$_1$). Let $\boldsymbol{H} = \sigma_0 \boldsymbol{u}_0 \boldsymbol{v}_0^\mathrm{T}$ and $\widehat{\boldsymbol{H}} = \sigma \boldsymbol{u} \boldsymbol{v}^\mathrm{T} + \sum_{j=2}^n \sigma_j \boldsymbol{u}_j \boldsymbol{v}_j^\mathrm{T}$ respectively denote singular value decompositions, where σ is the largest singular value of the matrix $\widehat{\boldsymbol{H}}$ (in agreement with step (S3) of the algorithm). Let $\boldsymbol{Z}$ denote the reconstruction error matrix, so that

$$\boldsymbol{Z} = \boldsymbol{H} - \widehat{\boldsymbol{H}} = \sigma_0 \boldsymbol{u}_0 \boldsymbol{v}_0^\mathrm{T} - \sigma \boldsymbol{u} \boldsymbol{v}^\mathrm{T} - \sum_{j=2}^n \sigma_j \boldsymbol{u}_j \boldsymbol{v}_j^\mathrm{T}. \tag{5}$$

Both, the correctness of the proposed algorithm and the localization performance analysis follow from the theorem and lemma below.

Theorem 1. *Let $\boldsymbol{u}, \boldsymbol{u}_0, \boldsymbol{v}, \boldsymbol{v}_0, \sigma, \sigma_0$ be as described above and the bound $\big\|\boldsymbol{H} - \widehat{\boldsymbol{H}}\big\|_\mathrm{F} \le \zeta$ be satisfied. Then $\langle \boldsymbol{u}_0, \boldsymbol{u} \rangle \langle \boldsymbol{v}_0, \boldsymbol{v} \rangle \ge \eta(\sigma, \sigma_0, \zeta)$ where*

$$\eta(\sigma, \sigma_0, \zeta) \triangleq \left(1 - \frac{\sigma}{\sigma_0}\right) + \sqrt{\left(1 - \frac{\sigma}{\sigma_0}\right)^2 + \left(\frac{\sigma}{\sigma_0}\right)^2 - \left(\frac{\zeta}{\sigma_0}\right)^2}. \tag{6}$$

Lemma 1. *$\eta(\sigma, \sigma_0, \zeta) \ge \sqrt{1 - \zeta^2/\sigma^2}$ is satisfied under the assumptions of Theorem 1.*

The main purpose of Lemma 1 is to bound $\eta(\sigma, \sigma_0, \zeta)$ in terms of quantities that are known to the algorithm during execution, and this is utilized in Problem (P$_2$). We shall defer the proof of Lemma 1 to a future publication. Theorem 1 essentially utilizes error bounds on low-rank matrix completion and translates them into direction error bound on the estimated singular vectors. Thereafter, it is ideologically straightforward to compute localization error bounds both numerically (by solving Problem (P$_2$)) and analytically (see Section 3.4). Note that *all* the dependence on sample complexity has been captured in the quantity ζ. This level of abstraction also allows us to compare localization performance for different decay profiles under a fixed sampling budget that is high enough for all the decay profiles in question.

3.3. Proof of Theorem 1

We let $\boldsymbol{P_u} = \boldsymbol{u}\boldsymbol{u}^{\mathrm{T}}$ and $\boldsymbol{P_v} = \boldsymbol{v}\boldsymbol{v}^{\mathrm{T}}$ respectively denote the matrices projecting onto the vectors $\boldsymbol{u}$ and $\boldsymbol{v}$, and let $\boldsymbol{P}_{\boldsymbol{u}^\perp} = \mathbf{I} - \boldsymbol{P_u}$ and $\boldsymbol{P}_{\boldsymbol{v}^\perp} = \mathbf{I} - \boldsymbol{P_v}$ denote the projection matrices onto the respective orthogonal complement spaces. We have,

$$\|\boldsymbol{Z}\|_{\mathrm{F}}^2 = \|(\boldsymbol{P_u} + \boldsymbol{P}_{\boldsymbol{u}^\perp})\boldsymbol{Z}(\boldsymbol{P_v} + \boldsymbol{P}_{\boldsymbol{v}^\perp})\|_{\mathrm{F}}^2 \tag{7a}$$
$$= \|\boldsymbol{P_u Z P_v} + \boldsymbol{P_u Z P}_{\boldsymbol{v}^\perp} + \boldsymbol{P}_{\boldsymbol{u}^\perp}\boldsymbol{Z P_v} + \boldsymbol{P}_{\boldsymbol{u}^\perp}\boldsymbol{Z P}_{\boldsymbol{v}^\perp}\|_{\mathrm{F}}^2 \tag{7b}$$
$$= \|\boldsymbol{P_u Z P_v}\|_{\mathrm{F}}^2 + \|\boldsymbol{P_u Z P}_{\boldsymbol{v}^\perp}\|_{\mathrm{F}}^2 + \|\boldsymbol{P}_{\boldsymbol{u}^\perp}\boldsymbol{Z P_v}\|_{\mathrm{F}}^2 + \|\boldsymbol{P}_{\boldsymbol{u}^\perp}\boldsymbol{Z P}_{\boldsymbol{v}^\perp}\|_{\mathrm{F}}^2 \tag{7c}$$
$$\geq \|\boldsymbol{P_u Z P_v}\|_{\mathrm{F}}^2 + \|\boldsymbol{P_u Z P}_{\boldsymbol{v}^\perp}\|_{\mathrm{F}}^2 + \|\boldsymbol{P}_{\boldsymbol{u}^\perp}\boldsymbol{Z P_v}\|_{\mathrm{F}}^2. \tag{7d}$$

where (7c) follows from (7b) since each term within the $\|\cdot\|_{\mathrm{F}}^2$ expression in (7b) is orthogonal to the other three terms *w.r.t.* the standard trace inner product over the vector space of $n \times n$ real matrices. We can evaluate each of the terms on the *r.h.s.* of (7d) as below.

$$\|\boldsymbol{P_u Z P_v}\|_{\mathrm{F}} = \left\|(\sigma_0\langle\boldsymbol{u}_0, \boldsymbol{u}\rangle\langle\boldsymbol{v}_0, \boldsymbol{v}\rangle - \sigma)\boldsymbol{u}\boldsymbol{v}^{\mathrm{T}} + \mathbf{0}\right\|_{\mathrm{F}} = |\sigma_0\langle\boldsymbol{u}_0, \boldsymbol{u}\rangle\langle\boldsymbol{v}_0, \boldsymbol{v}\rangle - \sigma|. \tag{8a}$$

$$\|\boldsymbol{P_u Z P}_{\boldsymbol{v}^\perp}\|_{\mathrm{F}} = \left\|\sigma_0\langle\boldsymbol{u}_0, \boldsymbol{u}\rangle\boldsymbol{u}\boldsymbol{v}_0^{\mathrm{T}}\boldsymbol{P}_{\boldsymbol{v}^\perp} + \mathbf{0}\right\|_{\mathrm{F}}$$
$$= |\langle\boldsymbol{u}_0, \boldsymbol{u}\rangle|\sigma_0\left\|\boldsymbol{v}_0^{\mathrm{T}}\boldsymbol{P}_{\boldsymbol{v}^\perp}\right\|_{\mathrm{F}} = |\langle\boldsymbol{u}_0, \boldsymbol{u}\rangle|\sigma_0\|\boldsymbol{P}_{\boldsymbol{v}^\perp}(\boldsymbol{v}_0)\|_{\mathrm{F}}$$
$$= |\langle\boldsymbol{u}_0, \boldsymbol{u}\rangle|\sigma_0\sqrt{1 - |\langle\boldsymbol{v}_0, \boldsymbol{v}\rangle|^2}. \tag{8b}$$

$$\|\boldsymbol{P}_{\boldsymbol{u}^\perp}\boldsymbol{Z P_v}\|_{\mathrm{F}} = \left\|\sigma_0\boldsymbol{P}_{\boldsymbol{u}^\perp}(\boldsymbol{u}_0)\langle\boldsymbol{v}_0, \boldsymbol{v}\rangle\boldsymbol{v}^{\mathrm{T}} + \mathbf{0}\right\|_{\mathrm{F}} \tag{8c}$$
$$= |\langle\boldsymbol{v}_0, \boldsymbol{v}\rangle|\sigma_0\|\boldsymbol{P}_{\boldsymbol{u}^\perp}(\boldsymbol{u}_0)\|_{\mathrm{F}} = |\langle\boldsymbol{v}_0, \boldsymbol{v}\rangle|\sigma_0\sqrt{1 - |\langle\boldsymbol{u}_0, \boldsymbol{u}\rangle|^2}.$$

For brevity of notation we let $\alpha = \langle\boldsymbol{u}_0, \boldsymbol{u}\rangle \leq 1$ and $\beta = \langle\boldsymbol{v}_0, \boldsymbol{v}\rangle \leq 1$. From the assumptions of the theorem, $\|\boldsymbol{Z}\|_{\mathrm{F}} \leq \zeta$ and combining this with (7) and (8) implies

$$\zeta^2 \geq (\sigma_0\alpha\beta - \sigma)^2 + \sigma_0^2\alpha^2(1 - \beta^2) + \sigma_0^2\beta^2(1 - \alpha^2) \tag{9a}$$
$$= \sigma^2 - 2\sigma\sigma_0\alpha\beta - \sigma_0^2\alpha^2\beta^2 + \sigma_0^2(\alpha^2 + \beta^2) \tag{9b}$$
$$\geq \sigma^2 - 2\sigma\sigma_0\alpha\beta - \sigma_0^2\alpha^2\beta^2 + 2\sigma_0^2|\alpha\beta|, \tag{9c}$$

where (9c) was obtained from (9b) using the relation $\alpha^2 + \beta^2 \geq 2|\alpha\beta|$. Because the signs of $\boldsymbol{u}$ and $\boldsymbol{v}$ can be switched globally without changing the estimate $\sigma\boldsymbol{u}\boldsymbol{v}^{\mathrm{T}}$, *w.l.o.g.* we assume $\alpha = \langle\boldsymbol{u}, \boldsymbol{u}_0\rangle \gtrsim 0$. We have

$$\sigma_0^2\alpha^2\beta^2 + 2\sigma_0\alpha(\sigma\beta - \sigma_0|\beta|) + \zeta^2 - \sigma^2 \geq 0, \tag{10}$$

which is a quadratic inequality in $\alpha\beta$ and hence, using the quadratic formula we get

$$\alpha \geq (\sigma_0\beta^2)^{-1}\left[(\sigma_0|\beta| - \sigma\beta) + \sqrt{(\sigma_0|\beta| - \sigma\beta)^2 - \beta^2(\zeta^2 - \sigma^2)}\right]. \tag{11}$$

Since $\alpha \leq 1$, (11) has a solution only if $\beta > 0$ and yields the joint bound

$$\alpha\beta \geq \left(1 - \frac{\sigma}{\sigma_0}\right) + \sqrt{\left(1 - \frac{\sigma}{\sigma_0}\right)^2 + \left(\frac{\sigma}{\sigma_0}\right)^2 - \left(\frac{\zeta}{\sigma_0}\right)^2}, \tag{12}$$

thus proving the theorem.

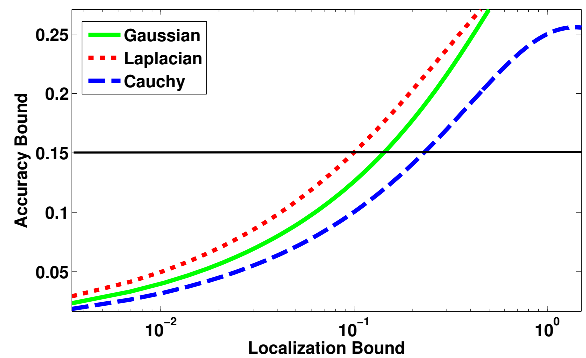

Fig. 2. Tradeoff showing the (continuous) Localization Bound l^{R} achievable for a given Accuracy Bound $\sqrt{1 - \zeta^2/\sigma^2}$ (and hence for a given sampling budget) for standard Gaussian, Laplacian and Cauchy fields.

3.4. Numerical Results

It is instructive to study the localization bound vs. accuracy trade-off for some known decay profiles from the exponential and power law families. Figure 2 shows the results for the standard Gaussian, Laplacian ($F(x) = 0.5\exp(-|x|)$) and Cauchy ($F(x) = 1/(\pi + \pi x^2)$) fields, using the continuous analogue of Problem (P_2), *i.e.* $\boldsymbol{v}$ is considered as the discretization of a one dimensional continuous function. For the fields mentioned, a closed form solution exists and takes the form of

$$l^{\mathrm{R}} = -l^{\mathrm{L}} = \sup\left\{l \;\middle|\; \frac{1}{\sqrt{l}}\int_0^l F(x)dx \geq \sqrt{1 - \zeta^2/\sigma^2}\right\}. \tag{13}$$

We see that for a given accuracy level $\sqrt{1 - \zeta^2/\sigma^2}$ (which translates to a fixed sampling budget), the Laplacian field admits the best localization bound l^{R}. This is somewhat surprising at first sight since Gaussian fields are inherently far more localized than Laplacian fields. However, the same phenomenon was confirmed via simulation experiments in [3]. Intuitively, good localization requires the right balance of "spread" and support of the "gradient" of the field which seems to be better in case of Laplacian fields and hence they show the best localization performance for a given sample complexity budget.

4. CONCLUSIONS

In this paper, we presented a target localization strategy from incomplete samples of the induced field. An algorithm was presented that exploited separability of the decaying field around the target to use a low-rank matrix completion based approach accompanied by a reduction in sample complexity of target detection. Knowledge of exact decay profiles was shown to be unnecessary. We also derived theoretical performance guarantees for the proposed algorithm and demonstrated a somewhat surprising phenomenon that Laplacian fields achieve better localization vs accuracy trade-off under a fixed sampling budget, as compared to Gaussian or Cauchy fields. As a matter of future work, we plan to relax the assumption of strict field decay to consider decaying envelopes and also investigate robust approaches to handle imaging artifacts like those in Figure 1.

References

[1] D. L. Donoho, "Compressed Sensing," *IEEE Trans. Inf. Theory*, vol. 52, no. 4, pp. 1289–1306, 2006.

[2] E. J. Candes and Y. Plan, "Matrix Completion With Noise," *Proc. IEEE*, vol. 98, no. 6, pp. 925–936, 2010.

[3] S. Choudhary, N. Kumar, S. Narayanan, and U. Mitra, "Active Target Detection with Mobile Agents," in *2014 IEEE International Conference on Acoustics, Speech and Signal Processing (ICASSP)*, May 2014, pp. 4218–4222.

[4] S. Choudhary, D. Kartik, N. Kumar, S. Narayanan, and U. Mitra, "Active Target Detection with Navigation Costs: A Randomized Benchmark," in *52nd Annual Allerton Conference on Communication, Control, and Computing (Allerton)*, Oct. 2014.

[5] B. Bhanu, "Automatic Target Recognition: State of the Art Survey," *Aerospace and Electronic Systems, IEEE Transactions on*, vol. AES-22, no. 4, pp. 364–379, Jul. 1986.

[6] T. Aridgides, D. Antoni, M. F. Fernandez, and G. J. Dobeck, "Adaptive filter for mine detection and classification in side-scan sonar imagery," in *SPIE's 1995 Symposium on OE/Aerospace Sensing and Dual Use Photonics*. International Society for Optics and Photonics, 1995, pp. 475–486.

[7] J. C. Hyland and G. J. Dobeck, "Sea mine detection and classification using side-looking sonar," in *SPIE's 1995 Symposium on OE/Aerospace Sensing and Dual Use Photonics*. International Society for Optics and Photonics, 1995, pp. 442–453.

[8] V. Chandola, A. Banerjee, and V. Kumar, "Anomaly Detection: A Survey," *ACM Comput. Surv.*, vol. 41, no. 3, pp. 15:1–15:58, Jul. 2009.

[9] P. F. Schweizer and W. Petlevich, "Automatic Target Detection and Cuing System for an Autonomous Underwater Vehicle (auv)," in *Unmanned Untethered Submersible Technology, 1989. Proceedings of the 6th International Symposium on*, Jun. 1989, pp. 359–371.

[10] E. Dura, Y. Zhang, X. Liao, G. J. Dobeck, and L. Carin, "Active learning for detection of mine-like objects in side-scan sonar imagery," *Oceanic Engineering, IEEE Journal of*, vol. 30, no. 2, pp. 360–371, 2005.

[11] S. Reed, Y. Petillot, and J. Bell, "An automatic approach to the detection and extraction of mine features in sidescan sonar," *Oceanic Engineering, IEEE Journal of*, vol. 28, no. 1, pp. 90–105, 2003.

[12] K. Mukherjee, S. Gupta, A. Ray, and S. Phoha, "Symbolic analysis of sonar data for underwater target detection," *Oceanic Engineering, IEEE Journal of*, vol. 36, no. 2, pp. 219–230, 2011.

[13] N. Kumar, Q. F. Tan, and S. S. Narayanan, "Object classification in sidescan sonar images with sparse representation techniques," in *Acoustics, Speech and Signal Processing (ICASSP), 2012 IEEE International Conference on*. IEEE, Mar. 2012, pp. 1333–1336.

[14] G. Hollinger, S. Choudhary, P. Qarabaqi, C. Murphy, U. Mitra, G. Sukhatme, M. Stojanovic, H. Singh, and F. Hover, "Underwater Data Collection Using Robotic Sensor Networks," *IEEE J. Sel. Areas Commun.*, vol. 30, no. 5, pp. 899–911, 2012.

[15] N. K. Yilmaz, "Path planning of autonomous underwater vehicles for adaptive sampling," Ph.D. dissertation, Massachusetts Institute of Technology, 2005.

[16] F. Bourgault, T. Furukawa, and H. F. Durrant-Whyte, "Optimal Search for a Lost Target in a Bayesian World," in *Field and Service Robotics*, ser. Springer Tracts in Advanced Robotics. Springer Berlin Heidelberg, 2006, vol. 24, pp. 209–222.

[17] L. Mihaylova, T. Lefebvre, H. Bruyninckx, K. Gadeyne, and J. De Schutter, "A Comparison of Decision Making Criteria and Optimization Methods for Active Robotic Sensing," in *Numerical Methods and Applications*, ser. Lecture Notes in Computer Science, I. Dimov, I. Lirkov, S. Margenov, and Z. Zlatev, Eds. Springer Berlin Heidelberg, 2003, vol. 2542, pp. 316–324.

[18] R. Hummel, S. Poduri, F. Hover, U. Mitra, and G. Sukhatme, "Mission design for compressive sensing with mobile robots," in *Robotics and Automation (ICRA), 2011 IEEE International Conference on*, May 2011, pp. 2362–2367.

[19] I. Bekkerman and J. Tabrikian, "Target Detection and Localization Using MIMO Radars and Sonars," *Signal Processing, IEEE Transactions on*, vol. 54, no. 10, pp. 3873–3883, Oct. 2006.

[20] D. Kalogerias, S. Sun, and A. Petropulu, "Sparse sensing in colocated MIMO radar: A matrix completion approach," in *Signal Processing and Information Technology(ISSPIT), 2013 IEEE International Symposium on*, Dec. 2013, pp. 496–502.

[21] D. S. Kalogerias and A. P. Petropulu, "Matrix completion in colocated MIMO radar: recoverability, bounds & theoretical guarantees," *IEEE Trans. Signal Process.*, vol. 62, no. 2, pp. 309–321, 2014.

[22] S. Sun, A. Petropulu, and W. Bajwa, "Target estimation in colocated MIMO radar via matrix completion," in *Acoustics, Speech and Signal Processing (ICASSP), 2013 IEEE International Conference on*, May 2013, pp. 4144–4148.

[23] D. Gross, "Recovering Low-Rank Matrices From Few Coefficients in Any Basis," *IEEE Trans. Inf. Theory*, vol. 57, no. 3, pp. 1548–1566, 2011.

[24] S. Negahban and M. J. Wainwright, "Restricted Strong Convexity and Weighted Matrix Completion: Optimal Bounds with Noise," *J. Mach. Learn. Res.*, vol. 13, no. 1, pp. 1665–1697, May 2012.

[25] J. Haupt, R. M. Castro, and R. Nowak, "Distilled sensing: Adaptive sampling for sparse detection and estimation," *IEEE Transactions on Information Theory*, vol. 57, pp. 6222–6235, September 2011.

[26] J. Haupt, R. Baraniuk, R. Castro, and R. Nowak, "Sequentially designed compressed sensing," in *Proc. IEEE Statistical Signal Processing Workshop*, Aug. 2012, pp. 401–404.

[27] M. Malloy and R. Nowak, "Near-optimal adaptive Compressed Sensing," in *Signals, Systems and Computers (ASILOMAR), 2012 Conference Record of the Forty Sixth Asilomar Conference on*, Nov. 2012, pp. 1935–1939.

[28] E. Balas, "Projection, lifting and extended formulation in integer and combinatorial optimization," *Ann. Oper. Res.*, vol. 140, pp. 125–161, 2005.

[29] S. Boyd and L. Vandenberghe, *Convex Optimization*. Cambridge University Press, 2004.